ELSEVIER

Bone Vol. 23, No. 3
September 1998:275–281

Intracortical Remodeling in Adult Rat Long Bones After Fatigue Loading

V. BENTOLILA,[1] T. M. BOYCE,[1] D. P. FYHRIE,[1] R. DRUMB,[1] T. M. SKERRY,[2] and M. B. SCHAFFLER[1,3]

[1] *Breech Research Laboratory, Bone and Joint Center, Henry Ford Health Sciences Center, Detroit, MI, USA*
[2] *Department of Biology, University of York, York, UK*
[3] *Department of Orthopaedics, The Mount Sinai School of Medicine, New York, NY, USA*

Intracortical remodeling in the adult skeleton removes and replaces areas of compact bone that have sustained microdamage. Although studies have been performed in animal species in which there is an existing baseline of remodeling activity, laboratory rodents have been considered to have limited suitability as models for cortical bone turnover processes because of a lack of haversian remodeling activity. Supraphysiological cyclic axial loading of the ulna in vivo was used to induce bending with consequent fatigue and microdamage. Right ulnae of adult Sprague-Dawley rats were fatigue-loaded to a prefailure stopping point of 30% decrease in ulnae whole bone stiffness. Ten days after the first loading, left ulnae were fatigued in the same way. Ulnae were harvested immediately to allow comparison of the immediate response of the left ulna to the fatigue loads, and the biological response of the right leg to the fatigue challenge. Histomorphometry and confocal microscopy of basic fuchsin-stained bone sections were used to assess intracortical remodeling activity, microdamage, and osteocyte integrity. Bone microdamage (linear microcracks, as well as patches of diffuse basic fuchsin staining within the cortex) occurred in fatigue-loaded ulnar diaphyses. Ten days after fatigue loading, intracortical resorption was activated in ulnar cortices. Intracortical resorption occurred in preferential association with linear-type microcracks, with microcrack number density reduced almost 40% by 10 days after fatigue. Resorption spaces were also consistently observed within areas of the cortex in which no bone matrix damage could be detected. Confocal microscopy studies showed alterations of osteocyte and canalicular integrity around these resorption spaces. These studies reveal that: (1) rat bone undergoes intracortical remodeling in response to high levels of cyclic strain, which induce microdamage in the cortex; and (2) intracortical resorption is associated both with bone microdamage and with regions of altered osteocyte integrity. From these studies, we conclude that rats can initiate haversian remodeling in long bones in response to fatigue, and that osteocyte death or damage may provide one of the stimuli for this process. (Bone 23:275–281; 1998)

Address for correspondence and reprints: Dr. Mitchell B. Schaffler, Department of Orthopaedics, The Mount Sinai School of Medicine, One Gustave Levy Place, Box 1188, New York, NY 10029.

Key Words: Bone remodeling; Fatigue; Bone microdamage; Osteocytes; Rat.

Introduction

Intracortical remodeling in the adult skeleton removes and replaces areas of compact bone that have sustained bone microdamage as a consequence of fatigue.[7,8,17,18,24,26] Left undetected and unrepaired, the accumulation of microdamage in bone leads to compromised mechanical properties and bone fragility. Microdamage accumulation due to an imbalance between damage-causing processes and intrinsic repair processes underlies the development of stress fractures[7,30] and may play a significant role in the increased bone fragility associated with aging and osteoporosis.[39,40] Bone microdamage and fragility are also implicated in bone implant failure and fractures associated with long-term usage of drugs that suppress bone remodeling physiology.[7] Recently, with the introduction of wide clinical usage of drugs that reduce bone remodeling globally in the skeleton, concerns have been raised about long-term pharmacological inhibition of bone remodeling leading to accumulation of unremodeled matrix damage, resulting in increased bone fragility in the population.[31] Accordingly, examination of factors that influence microdamage accumulation in the skeleton, and those factors that influence its detection and repair, are fundamental to understanding skeletal health and disease.

There have been few experimental studies of the relationship between bone microdamage and intrinsic repair processes, owing in part to an incomplete understanding of bone fatigue and resulting bone matrix damage processes, and in part to the inherent difficulty and expense of performing these studies in vivo. Numerous studies over the last several years have shown that bone fatigues quite readily with normal mechanical usage, with fatigue microdamage occurring at multiple levels of the bone microarchitecture.[4,5,7,16,39,40] The few previous experimental studies examining whether intracortical remodeling in the adult skeleton removes and replaces microdamaged areas of compact bone were performed in dogs, because canine bone, like human bone, is osteonal and has an existing baseline of intracortical remodeling activity.[8,26] However, it is unknown whether repair of microdamage through remodeling is characteristic only of haversian bone, or whether bone fatigue will similarly activate osteonal remodeling processes to effect matrix repair in a species within which intracortical turnover is characteristically absent. In the current study, we tested the hypothesis that bone fatigue loading in vivo can activate the remodeling process in bones in

8756-3282/98/$19.00
PII S8756-3282(98)00104-5

Bone Vol. 23, No. 3
September 1998:275–281

which haversian remodeling characteristically does not occur. Accordingly, the objectives of the current studies were to develop a system by which adult rat long bones could be fatigued in vivo, and to use that system to determine whether fatigue loading in vivo would activate intracortical remodeling in adult rat long bones.

Materials and Methods

The end-load ulnar bending system[43] was adapted for use as an in vivo fatigue loading system. This system applies axial loads to the ends of the ulna resulting in bending moment in the ulnar diaphysis. End-load bending of rat ulnae results in bone strains distributed in the ulnar diaphysis as tension on the medial ulnar surface, a neutral axis within the bone, and compression on the lateral ulnar surface.[43] It has been used widely to examine bone modeling in small, growing animals.[15,19,29,43] We adapted the loading system for use in 16 adult Sprague-Dawley rats, 5 months old, weighing 350 ± 25 g (Charles River). During loading, rats were anesthetized using isoflurane (0.5–3%) inhalation. The loading period was limited to a maximum of 3 h (i.e., 43,200 cycles) due to anesthesia safety concerns. Body temperature was maintained using a recirculating heating pad. Before and after loading, animals were allowed unrestricted cage activity and ad libitum access to food and water. Procedures were conducted with approval from the governing animal care committee of the Henry Ford Health Sciences Center.

Loads were applied using a constant-load, cam-driven device, constructed in our laboratory. During loading, the forelimb was positioned in the apparatus with the elbow and volar flexed carpus placed in padded brass cups. Loads were measured using a 50-lb. load cell (Model #31, Sensotec, Cleveland, OH). Axial displacement range was measured using an LVDT (Model #DLB1000, Sensotec). Load and displacement were recorded using A/D data acquisition. At the start of each experiment, the limb cycled for 100 cycles with a small (1 N) preload to allow it to settle into position. Fatigue loading was then performed using a 20 N maximum load range, which corresponds to approximately 4000 microstrain (SD: ± 495 microstrain) on the ulnar diaphyseal surface.[3] Cyclic loading was conducted at 4 Hz. Ulnae were fatigued to a single stopping point based on loss of bone stiffness.[1,4,10–12,32,37,38,41] Fatigue-induced losses of ulnar structural stiffness were determined from increases in ulnar compliance, defined as the increase in absolute displacement range (maximum − minimum) during cyclic loading. Right ulnae of rats were fatigue-loaded to a prefailure stopping point of 30% decrease in ulnae whole bone stiffness. After loading, animals were returned to their cages; animals recovered quickly and ambulated normally after loading. Ten days after the first loading, left ulnae were fatigued in the same way. Rats were killed immediately after the second loading session, without recovery from anesthesia. Ulnae were harvested immediately to allow comparison of the immediate response of left ulna to the fatigue loads (acute fatigue), and the biological response of right legs to the fatigue challenge (fatigue/survival). In addition, a group of nonloaded ulnae from a group of untreated baseline animals were examined as histological controls for microdamage and osteocyte integrity.

At necropsy, both forelimbs were manually dissected free of soft tissues and processed for histological analysis. Forearm bones (radius-ulna) were stained en bloc in 1% basic fuchsin in ethanol to differentially show microdamage.[9,17] After embedding in methylmethacrylate, undecalcified diaphyseal cross sections were cut serially through the middle third of the diaphysis using a diamond wafering saw, ground to 50 μm, mounted on glass slides, and coverslipped for microscopic analysis. Histomorphometric analyses were performed using bright-field microscopy. Point count stereological methods using a 10 mm × 10 mm eyepiece grid reticule and 25× objective magnification were used to determine bone cross-sectional area (B.Ar, mm^2), intracortical resorption space number density (Rs.Dn, #/mm^2), and area (Rs.Ar, mm^2). Microdamage content was measured from number density of typical linear microcracks (Cr.Dn, #/mm^2) and from area occupied by patches of diffuse basic fuchsin staining within the cortex (Df.dx, mm^2), following the methods of Boyce et al.[5] and Schaffler et al.[37] Intracortical resorption spaces were categorized as to whether or not they occurred in association with bone microdamage, with association defined as a resorption space being adjacent to or intersecting with a damage focus. Overall osteocyte number density (Ot.Dn, #/mm^2) and atypical-appearing osteocyte number (A-Ot.Dn, defined as lacunae with shrunken cells, "empty" lacunae, and cells with pyknotic nuclei) (**Figure 1**) were determined from each section as an indirect measure of osteocyte integrity. This broad definition was used because of the potential uncertainties that exist when distinguishing empty lacunae from lacunae having osteocytes with condensed cytoplasm, using thick sections of bone.[14,44] Atypical-appearing osteocyte number was determined in nonremodeling areas of bone and within one complete grid-field area (0.160 mm^2) surrounding each resorption space. Histomorphometric data were collected by a single, observer (V.B.), with cross checking of randomly chosen sections by a second observer (M.B.S.); agreement between observers was within 5%.

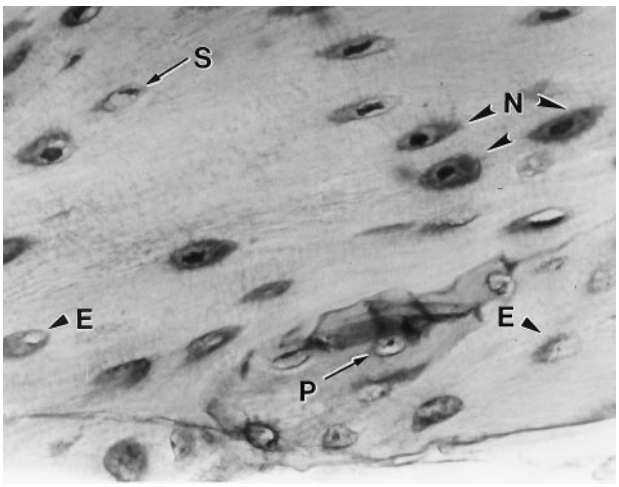

Figure 1. Bright-field photomicrograph showing normal and atypical osteocyte morphology in rat ulnar cortex. N, normal osteocytes; S, shrunken osteocyte, retracted against lacunar wall; P, osteocyte with pyknotic nucleus; E, "empty" lacuna (i.e., a lacuna containing no discrete cell or nucleus). Photomicrograph field width 280 μm.

Confocal microscopy was used for detailed morphological studies.[5,41] Specimens were observed using a BioRad 1024 laser-scanning confocal microscope (BioRad, Herts., UK) equipped with a krypton-argon laser, mounted on a Zeiss Axiovert microscope base. Specimens were viewed using 568 nm wavelength excitation and a 605 nm DF35 emission filter to take advantage of the fluorescence of basic fuchsin and to eliminate background autofluorescense of the bone. Observations were made using 40× (numerical aperture 1.3) and 63× (numerical aperture 1.4) magnification oil-immersion objectives.

These studies were undertaken using a paired design, with secondary internal comparisons within fatigue/survival limbs. Independent (nonloaded) control tissues served only to establish the baseline for histological processing effects and were not

Table 1. Summary histomorphometric data for experimentally loaded ulnar diaphyses (data expressed as mean ± SD)

Parameter	Limb treatment		Significance[a]
	Acute fatigue	Fatigue/survival	
B.Ar (mm^2)	2.02 ± 0.18	2.12 ± 0.19	$p > 0.60$
Cr.Dn (#/mm^2)	3.39 ± 1.71	2.10 ± 0.77	$p < 0.05$
Df.dx (mm^2)	0.91 ± 0.53	0.71 ± 0.25	$p > 0.15$
Rs.Dn (#/mm^2)	0	1.46 ± 0.59	$p < 0.0001$
Rs.Ar (mm^2)	0	0.031 ± 0.003	$p < 0.0001$

Abbreviations: B.Ar, bone area; Cr.Dn, microcrack density; Df.dx, diffuse damage area; Rs.Dn, resorption space density; Rs.Ar, mean resorption space area.
[a]Determined using Wilcoxon signed-rank test, comparing acute fatigue vs. fatigue/survival ulnae.

included in the statistical analyses of experimental data. Statistical comparisons of acute fatigue vs. fatigue/survival limbs were performed between limbs within the same animals using the Wilcoxon signed-rank test. Among fatigue/survival limbs, chi-square one-sample analysis was used to test whether the frequency of associations between resorption spaces and bone microdamage type differed from those expected due to random association. In addition, within fatigue/survival limbs, Kendall's rank correlation (τ) was calculated to determine the significance of associations between resorption parameters (number and area), amounts of bone microdamage, and osteocyte integrity. Statistical analyses were performed using the StatView version 4.5 software package (Abacus Concepts, Berkeley, CA). Data are reported as mean ± standard deviation.

Results

Gross Observations and Fatigue Behavior of Rat Ulnae

Ulnae in 14 of 16 animals were fatigued successfully to the specified experimental endpoint. Average number of cycles for specimens to reach the fatigue stopping point of 30% change in ulnar compliance was 8853 ± 4201 cycles. Loading was stopped after 3 h for two animals in which the target fatigue level was not achieved by that time. Between limbs within the same animal, there was no significant difference in the number of load cycles needed to reach the defined endpoint. At necropsy, acute fatigue ulnae appeared grossly normal. Some fatigue/survival ulnae showed a hyperemic region in the midulnar diaphysis. Periosteal reaction was not routinely observed grossly.

Histological Observations

At 10 days after fatigue loading, some periosteal new bone formation was observed in the ulnar diaphyses, but its presence varied widely among animals. There were no significant increases in cortical bone areas for fatigue/survival vs. acute fatigue ulnae ($p > 0.6$). Data for cortical bone areas are summarized in **Table 1**.

Bone microdamage. Bone matrix microdamage was observed in all fatigue-loaded ulnar diaphyses. Microdamage was present as ultrastructural matrix damage, evidenced by patches of diffuse basic fuchsin staining within the cortex, and as linearly stained microcracks (**Figures 2 and 3**). Microdamage occurred principally in medial and lateral (tensile and compressive) ulnar cortices. Microdamage was not observed in nonloaded control bones. In addition, microdamage was not seen in radial diaphyses from loaded limbs, consistent with the expectation that the radius would not receive a significant load when forces are applied to the carpal and olecranon ends of the ulna.

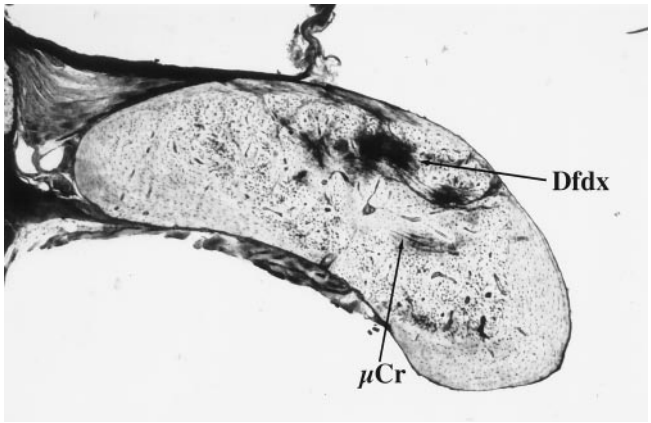

Figure 2. Cross section of acutely fatigued rat ulnar diaphysis, showing linear microcracks (μCr), and patches of uptake of basic fuchsin (Df.dx); these latter regions correspond to the increase permeability to basic fuchsin, due to sublamellar cracking. Photomicrograph field width 2.75 mm.

At 10 days after loading, microcrack density (Cr.Dn) was significantly lower, by almost 40% ($p < 0.05$), than in acute fatigue ulnae. The area occupied by patches of diffuse damage (Df.dx) was reduced at 10 days; however, this difference was not significant ($p > 0.15$). Data for Cr.Dn and Df.dx are summarized in Table 1.

Intracortical resorption. At 10 days after loading, intracortical resorption was activated in ulnar cortices in all fatigued limbs (Table 1 and Figure 3). Typical intracortical resorption spaces were observed within the ulnar cortex; tunneling canals from the endocortical and periosteal surface were seen as well (Figure 3). Resorption spaces were located principally in medial and lateral cortices. Intracortical resorption sites were not observed in the adjacent radial diaphyses from loaded limbs. Resorption sites were not seen in contralateral acute fatigue ulnae. Intracortical remodeling was absent from the ulnar cortices of the two animals for which large numbers of load cycles were administered without fatigue.

Intracortical remodeling occurred in preferential association

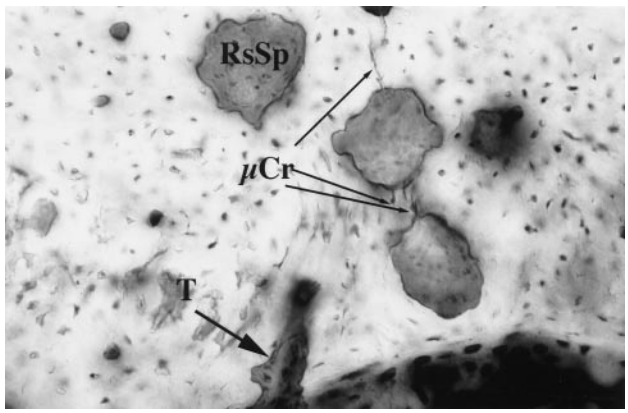

Figure 3. Cross section of rat ulnar diaphysis at 10 days after fatigue loading, showing several intracortical resorption spaces (Rs.Sp). Linear microcracks are seen in association with resorption spaces (μCr, arrows). Osteoclastic tunneling (T) from the periosteal surface can also be seen. Photomicrograph field width 560 μm.

Bone Vol. 23, No. 3
September 1998:275–281

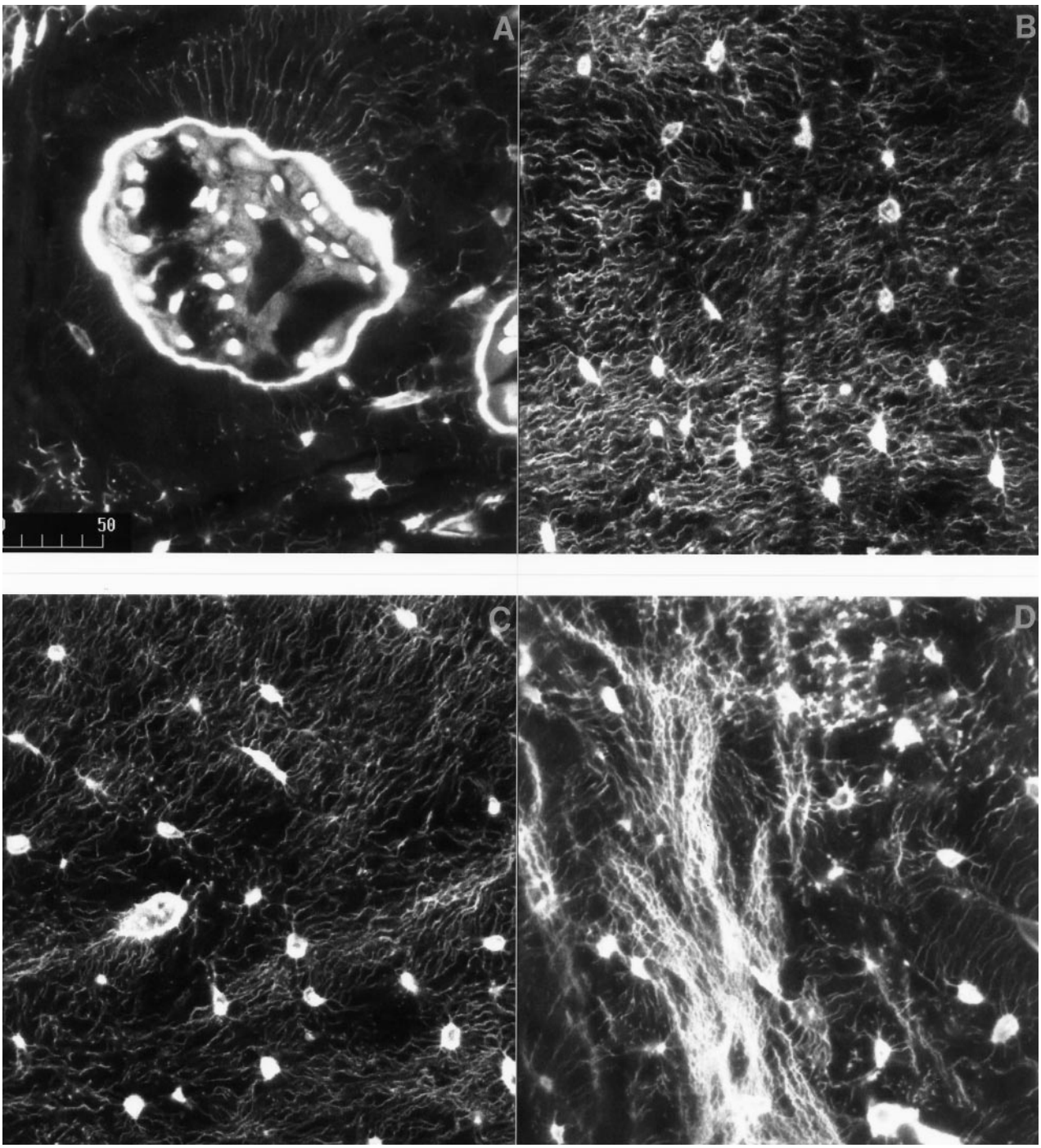

Figure 4. Confocal photomicrographs of basic fuchsin-stained cross sections from rat ulnar diaphyses. (A) Intracortical resorption space in the ulnar cortex 10 days after fatigue loading. Fewer osteocytes are observed, and canalicular staining in the regions undergoing resorption is dramatically reduced compared with the normal osteocyte and canalicular structure in control bone (B). (C) Normal appearance of osteocytes in bone 10 days after fatigue loading, from a region of bone not undergoing bone remodeling. (D) Normal appearance of osteocytes in diffusely damaged region of acutely fatigued bone. Scale bar 50 μm; photomicrograph field width 260 μm.

with linear-type bone microcracks ($p < 0.01$, Figure 2), with 74% of the microcracks observed in association with resorption spaces. In contrast, intracortical resorption was not significantly associated with diffusely damage foci ($p = 0.075$). However, resorption spaces were also seen within areas of the cortex in which no matrix damage could be detected. Confocal microscopy studies revealed that, for intracortical resorption spaces occurring in areas of bone for which no matrix damage was seen, osteocyte and canalicular integrity appeared to be impaired (**Figure 4**A). In adjacent areas of bone that were not being remodeled, normal lacunar and canalicular staining was observed (Figure 4B,C). Osteocyte staining appeared unaltered in bone from the acute

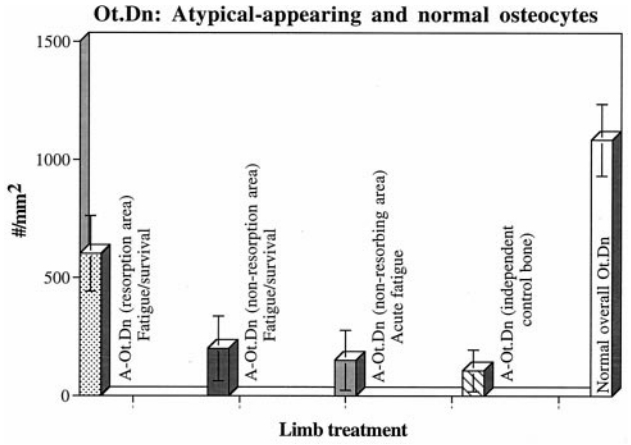

Figure 5. Summary data for atypical-appearing (A-Ot.Dn) and normal (Ot.Dn) osteocyte number densities for different regions in experimental bones; independent (nonloaded) control tissue are included for reference. A-Ot.Dn for independent control tissue and overall normal Ot.Dn are shown for reference. Data expressed as mean ± standard deviation. A-Ot.Dn in acutely fatigued bones was similar to that in independent control bones. A-Ot.Dn at 10 days after fatigue was significantly increased in bone surrounding resorption spaces ($p < 0.01$). In adjacent nonresorbing areas within the same bones, A-Ot.Dn was not significantly different from that in acutely fatigued bones.

fatigue samples (Figure 4D). Resorption space number and size were highly significantly correlated with the number of linear-type microcracks ($\tau = 0.55$; $p < 0.03$; $\tau = 0.57$; $p < 0.02$, respectively). In contrast, there were no significant correlations between bone resorption parameters and the amount of diffuse damage in bone.

Osteocytes. Overall osteocyte density was equivalent in both acute fatigue and fatigue/survival ulnae. Low densities of atypical-appearing osteocytes (A-Ot.Dn) were observed in acute fatigue and independent control ulnae ($150 \pm 102/mm^2$ and $107 \pm 88/mm^2$, respectively). At 10 days after loading, A-Ot.Dn in nonresorbing areas within fatigue/survival bones was increased ($205 \pm 102/mm^2$), but not significantly over acute fatigue and control tissue. Around resorption sites, atypical-appearing osteocyte density was three- to four-fold higher ($602 \pm 152/mm^2$) than in nonresorbing areas within fatigue/survival ulnae or in acute fatigue bones ($p < 0.01$). Osteocyte density data are summarized in **Figure 5**. Resorption space size (Rs.Ar) was significantly correlated with the density of atypical-appearing osteocytes ($\tau = 0.55$; $p < 0.03$). Microcrack density and A-Ot.Dn were not well correlated ($\tau = 0.40$; $p < 0.065$).

Discussion

The current studies show that adult rat long bones can be fatigued in vivo, using a modification of the ulnar bending system.[43] The resulting bone microdamage patterns show diffuse-type sublamellar cracking and linear microcracks, consistent with observations of matrix failure modes in fatigued human and canine compact bone, which have been reported previously.[5,10,37,38] These results also show that cortical bone in the rat initiates intracortical resorption when the bones are fatigued in vivo. That rat bone is capable of remodeling in response to a physiological challenge is entirely consistent with the literature. Basic multicellular unit (BMU)-based remodeling occurs in rat cancellous bone[2] and in cortical bone in response to metabolic challenge, such as lactation and calcium deficiency.[3,20,23,25,36] Moderate increases in mechanical loading of rat long bones do not normally induce intracortical remodeling, but instead stimulate modeling changes on bone surfaces.[15,19,29,43] The current observation that intracortical remodeling is activated in association with fatigue loading is a novel finding in terms of mechanically induced changes in rat bone. We have shown that cortical bone in the rat initiates haversian remodeling where mechanical circumstances dictate that it is an appropriate response.

Intracortical resorption did not occur in the absence of fatigue in rat ulnae. There were two animals for which large numbers of load cycles were administered (some 43,000 cycles) without bone fatigue. These experiments were stopped after 3 h because of the length of time that the animals were anesthetized. Analyses of the forearm bones from these two animals indicated that they had larger cross-sectional dimensions, so the bending strains from loading in these bones would be expected to be lower than in other experimental animals, resulting in lower stresses and prolonged fatigue lives. However, the data from these animals are instructive in that they show that the activation of intracortical resorption process in rat long bone cortices is not a function of the large number of loading cycles to which experimental limbs are subjected. In the current studies, intracortical resorption was activated only in association with bone fatigue.

Microcracks in bone, observable as small cracks in bone matrix visible at the light-microscopic level, are thought to be the microstructural consequence of bone fatigue. Frost[17] reported the first observations of microdamage in bone in human rib samples. He described small cracks, with a "linear" morphology, typically on the order of 30–100 μm in length. Frost also hypothesized that osteonal remodeling would effect the repair of microcracks. Such typical linear microcracks have received much study. They have been produced experimentally by fatigue-loading bone in vivo[8,26] and in vitro.[5,12,37,38] However, there are other levels of matrix failure in bone, which occur early in the fatigue process, and strongly influence its fatigue behavior. Burr et al.[9] reported that whole bones in bending fatigue lost large amounts of stiffness before linear microcracks became apparent, indicating that other levels of matrix damage must account for early stiffness loss. Boyce et al.[5] and Schaffler et al.[37] demonstrated that bone fatigue results in focal patches of bone with increased permeability to stain. At higher magnification, these diffusely stained patches were comprised of very fine matrix microcracking at the sublamellar level. Similar matrix failure mechanisms were reported in the fracture toughness studies of Zioupos et al.[45] In the current studies, fatigue-loaded ulnae demonstrated a variety of matrix-level damage processes, with linear-type microcracks and patches of diffuse basic fuchsin staining being the predominant modes of matrix failure. Fatigue loading in the current experiments was conducted at a higher strain than would be expected for habitual physiological loading,[34,35] but this strain approximates that measured in racehorses during unrestricted track running.[30] It was chosen to assure completion of the entire experiment series within a reasonable time frame. However, with bone fatigue at the lower strains more characteristic of habitual usage, similar microdamage mechanisms have been shown to occur.[32,38]

Previous experimental studies on bone remodeling and microdamage physiology in vivo show that osteoclastic cutting cones are associated with remodeling of linear microcracks from canine compact bone.[8,26] The relationship of other levels of matrix failure in bone fatigue (i.e., diffuse matrix microdamage) to the osteonal remodeling/repair process in bone has been previously unexplored. In the current studies, intracortical resorption foci occurred in high association with linear microcracks, consistent with previous studies in canine bone. By 10 days, there were almost 40% fewer linear microcracks present than acutely after fatigue. In contrast, foci of diffuse damage

showed a weak association with resorption activity, with a commensurately smaller reduction in diffuse damage content after 10 days. The reason for this difference remains obscure at the present time. It may represent a difference in turnover/repair efficiency, such that normal intracortical resorption spaces are better "matched" in size for eliminating small, linear microcracks than larger patches of diffuse matrix damage. An alternative possibility is that the diffuse matrix damage itself invokes different local mechanisms for signaling, targeting, and effecting its repair than does linear-type microcracking.

The current studies indicate that, after fatigue loading, there was a marked increase in atypical-appearing osteocytes. This occurred in regions with and without detectable microdamage. Moreover, intracortical resorption spaces were also found in areas of bone for which osteocyte and canalicular integrity appeared to be impaired, but no matrix damage was observed. The biological nature of this osteocyte reaction to fatigue loading cannot be determined directly from the methods used in the current studies. En bloc staining of bones with basic fuchsin, as used in these experiments, is optimized to differentially stain bone microdamage. Osteocyte viability, which is best assessed from lactate dehydrogenase staining,[14,44] could not be directly characterized on the same tissues. In addition to bone microdamage, basic fuchsin also stains proteoglycans and glycoproteins. In bone, basic fuchsin stains osteocytes and their lacunae and canaliculi and, in the latter instance, is taken up by the nonmineralized organic layer that lines these structures.[13] Thus, loss of osteocyte, lacunar and canalicular staining, as observed in our confocal microscopy studies, is an indication that osteocyte function has been impaired. Similarly, the observed increases in atypical-appearing osteocytes in fatigue/survival bones shows that these cells have been altered in fatigue-loaded bone. However, these data do not provide a direct characterization of how osteocyte function has been affected. Previous studies have shown that, in thick ground sections of bone, such as those used in the current studies, empty osteocyte lacunae cannot be distinguished with certainty from lacunae having osteocytes with condensed cytoplasm.[14,44] This distinction may be critical, as the former represents dead tissue, whereas the latter is more characteristic of injured cells.[21] Nevertheless, although the nature of the osteocyte reaction to fatigue loading cannot be assessed directly from the methods used in the current studies, the present data show a significant increase in atypical osteocyte number by 10 days after fatigue. This alteration of osteocyte and canalicular integrity occurred with intracortical resorption spaces and microcracks, both individually and in association with each other, suggesting that changes in osteocyte integrity may represent a final common target for bone remodeling activity in response to fatigue loading.

It has been suggested that bone microdamage could cause osteocyte injury, thereby signaling remodeling of a region of bone.[17,18,22] However, until recently, there were no data to support this assertion. Qiu et al.[33] in our laboratory, showed that osteocyte apoptosis occurs in reaction to acutely induced matrix damage in bone, providing intriguing evidence to suggest that osteocyte apoptosis may be a critical step in the process by which damaged bone and osteocytes are signaled and targeted for removal by osteoclastic resorption. Association between osteocyte apoptosis and bone resorption has been shown in developing bone, and may be implicated in increased bone resorption after estrogen withdrawal.[6,28,29,42] Further studies are necessary to test whether similar mechanisms underlie the observed alterations of osteocyte integrity and their association with bone fatigue and remodeling, and thereby operate in targeting of bone turnover in response to fatigue. Data from the current studies support the idea that changes in osteocyte integrity, perhaps through local bone fatigue injury-induced apoptosis, are associated with activation, signaling to, or targeting of intracortical resorption processes after bone fatigue.

Acknowledgements: Portions of this work were presented at the 43rd annual meeting of the Orthopaedic Research Society. The authors are grateful to D. Lundin-Cannon for providing expert assistance with histological techniques, and A. M. Saad for assistance with instrumentation and mechanical measurements. The authors also thank Dr. Harold Frost, Dr. Gary Gibson, Dr. Steve Goldstein, and Dr. Eric Radin for their helpful comments. V. B. was supported in part by research training grants from the Assistance Publique des Hôpitaux de Paris and the Societé Français de Chirurgie Orthopédique ét Traumatologique. This research was supported by Grants AR41210 and AR40776 from the National Institute of Arthritis, Musculoskeletal and Skin Diseases.

References

1. Agarwal, B. D. and Broutman, L. J. Analysis and Performance of Fiber Composites. New York: Wiley; 1980.
2. Baron, R., Tross, R., and Vignery, A. Evidence of sequential remodeling in rat trabecular bone: Morphology, dynamic histomorphometry and changes during skeletal maturation. Anat Rec 208:137–145; 1984.
3. Bentolila, V., Hillam, R. A., Skerry, T., Boyce, T. M., Fyhrie, D. P., and Schaffler, M. B. Activation of intracortical remodeling in adult rat long bones by fatigue loading. Trans Orthop Res Soc 22:578; 1997.
4. Boyce, T. M., Fyhrie, D. P., Brodie, F. R., and Schaffler, M. B. Residual mechanical properties of human cortical bone following fatigue loading. Am Soc Biomech 20:23–24; 1996.
5. Boyce, T. M., Fyhrie, D. P., Radin, E. L., and Schaffler, M. B. Damage and strain mode associations in human compact bone bending fatigue. J Orthop Res. In press.
6. Bronckers, A. L. J. J., Goei, W., Luo, G., Karsenty, G., D-Souza, R. N., Lyaruu, D. M., and Burger, E. H. DNA fragmentation during bone formation in neonatal rodent assessed by transferase mediated end labeling. J Bone Miner Res 11:1281–1291; 1996.
7. Burr, D. B., Forwood, M. R., Schaffler, M. B., Fyhrie, D. P., Martin, R. B., and Turner, C. H. Bone microdamage and skeletal fragility in osteoporotic and stress fractures. J Bone Miner Res 12:6–15; 1997.
8. Burr, D. B., Martin, R. B., Schaffler, M. B., and Radin, E. L. Bone remodeling in response to *in vivo* fatigue microdamage. J Biomech 18:189–200; 1985.
9. Burr, D. B. and Stafford, T. Validation of the bulk-staining technique to separate artifactual from in vivo bone microdamage. Clin Orthop 260:305–309; 1991.
10. Carter, D. R., Caler, W. E., Spengler, D. M., and Frankel, V. H. Fatigue behavior of adult cortical bone: The influence of mean strain and strain range. Acta Orthop Scand 52:481–490; 1981.
11. Carter, D. R., Caler, W. E., Spengler, D. M., and Frankel, V. H. Uniaxial fatigue of human cortical bone: The influence of tissue physical characteristics. J Biomech 14:461–470; 1981.
12. Carter, D. R. and Hayes, W. C. Compact bone fatigue damage: A microscopic examination. Clin Orthop 127:265–274; 1977.
13. Doty, S. B., Robinson, R. A., and Schofield, B. Morphological and histochemical staining characteristics of bone cells. In: Aurbach, G. D., Ed., Handbook of Physiology. Washington, DC: American Society of Physiology; 1976; 3–23.
14. Dunstan, C. R., Somers, N. M., and Evans, R. A. Osteocyte death and hip fracture. Calcif Tissue Int 53(Suppl.):113–119; 1993.
15. Fermor, B. and Skerry, T. M. PTH/PTHrP receptor expression on osteoblasts and osteocytes but not resorbing bone surfaces in growing rats. J Bone Miner Res 10:1935–1943; 1995.
16. Forwood, M. R. and Parker, A. W. Microdamage in response to repetitive torsional loading in the rat tibia. Calcif Tissue Int 45:47–53; 1989.
17. Frost, H. M. Presence of microscopic cracks *in vivo* in bone. Henry Ford Med Bull 8:27–35; 1960.
18. Frost, H. M. Bone microdamage: Factors that impair its repair. In: Uhthoff, H. K., Ed. Current Concepts in Bone Fragility. Berlin: Springer; 1985.
19. Hillam, R. A. and Skerry, T. M. Inhibition of bone resorption and stimulation of formation by mechanical loading of the modeling rats ulna in vivo. J Bone Miner Res 10:683–689; 1995.
20. Jee, W. S. S., Mori, S., Li, X. J., and Chan, S. Prostaglandin E_2 enhances

cortical bone mass and activates intracortical bone remodeling in intact and ovariectomized female rats. Bone 11:253–266; 1990.
21. Kerr, J. F. R. and Harmon, B. V. Definition and incidence of apoptosis. In: Tomei, L. D. and Cope, F. O., Eds. Apoptosis: The Molecular Basis of Cell Death. Cold Spring Harbor, NY: Cold Spring Harbor; 1991; 5–30.
22. Lanyon, L. E. Osteocytes, strain detection and bone modeling and remodeling. Calcif Tissue Int 53(Suppl.):102–107; 1993.
23. Li, X. J., Jee, W. S. S., Ke, H. Z., Mori, S., and Akamine, T. Age-related changes of cancellous and cortical bone histomorphometry in female Sprague-Dawley rats. Scann Microsc Int (Cells Mater) (Suppl. 1):25–36; 1991.
24. Martin, R. B. and Burr, D. B. A hypothetical mechanism for the stimulation of osteonal remodeling by fatigue damage. J Biomech 15:137–139; 1982.
25. Miller, S. C., Shupe, J. G., Redd, E. H., Miller, M. A., and Omura, T. H. Changes in bone mineral and bone formation rates during pregnancy and lactation in rats. Bone 7:283–287; 1986.
26. Mori, S. and Burr, D. B. Increased intracortical remodeling following fatigue damage. Bone 14:103–109; 1993.
27. Mori, S., Harruff, R., Ambrosius, W., and Burr, D. B. Trabecular bone volume and microdamage accumulation in femoral heads of women with and without femoral neck fractures. Bone 21:521–526; 1997.
28. Noble, B. S., Stevens, H., Loveridge, N., and Reeve, J. Identification of apoptotic changes in osteocytes in normal and pathological human bone. Bone 20:273–282; 1997.
29. Noble, B. S., Stevens, H., Mosley, J. R., Pitsillades, A. A., Reeve, J., and Lanyon, L. Bone loading changes the number and distribution of apoptotic osteocytes in cortical bone. J Bone Miner Res 12(Suppl. 1):36; 1997.
30. Nunamaker, D. M., Butterweck, D. M., and Provost, T. M. Fatigue fractures in thoroughbred racehorses: Relationship with age, peak bone strain and training. J Orthop Res 8:604–611; 1990.
31. Parfitt, A. M., Mundy, G. R., Roodman, G. D., Hughes, D. E., and Boyce, B. F. A new model for the regulation of bone resorption with particular reference to the effect of bisphosphonates. J Bone Miner Res 11:150–159; 1996.
32. Pattin, C. A., Caler, W. E., and Carter, D. R. Cyclic mechanical property degradation during fatigue loading of cortical bone. J Biomech 29:69–79; 1996.
33. Qiu, S.-J., Hoshaw, S. J., Gibson, G. J., Lundin-Cannon, K. D., and Schaffler, M. B. Osteocyte apoptosis in reaction to matrix damage in compact bone. Trans Orthop Res Soc 22:89; 1997.
34. Rubin, C. T. Skeletal strain and the functional significance of bone architecture. Calcif Tissue Int 36(Suppl.):11–18; 1984.
35. Rubin, C. T. and Lanyon, L. E. Limb mechanics as a function of speed and gait: A study of functional strains in the radius and tibia of horse and dog. J Exp Biol 101:187–211; 1982.
36. Ruth, E. B. Bone studies II. An experimental study of the haversian type vascular channels. Am J Anat 93:429–455; 1953.
37. Schaffler, M. B., Boyce, T. M., and Fyhrie, D. P. Tissue and matrix failure modes in human compact bone during tensile fatigue. Trans Orthop Res Soc 21:57; 1996.
38. Schaffler, M. B., Burr, D. B., and Radin, E. L. Mechanical and morphological effects of strain rate on fatigue in compact bone. Bone 10:207–214; 1989.
39. Schaffler, M. B., Choi, K., and Milgrom, C. Aging and matrix microdamage accumulation in human compact bone. Bone 17:521–525; 1995.
40. Schaffler, M. B., Pitchford, W. C., Choi, K., and Riddle, J. M. Examination of compact bone microdamage using back-scattered electron microscopy. Bone 15:483–488; 1994.
41. Schaffler, M. B., Radin, E. L., and Burr, D. B. Long-term fatigue behavior of compact bone at low strain magnitude and rate. Bone 11:321–326; 1990.
42. Tomkinson, A., Reeve, J., Shaw, R. W., and Noble, B. S. The death of osteocytes via apoptosis accompanies estrogen withdrawal in human bone. J Clin Endocrinol Metab 82:3128–3135; 1997.
43. Torrance, A. G., Mosley, J. M., Suswillo, R. F. L., and Lanyon, L. E. Noninvasive loading of the rat ulna in vivo induces modeling response uncomplicated by periosteal trauma. Calcif Tissue Int 54:241–247; 1994.
44. Wong, S. Y. P., Dunstan, C. R., Evans, R. A., and Hills, E. The determination of bone viability: A histochemical methods for identification of lactate dehydrogenase activity in osteocytes in fresh and decalcified sections of human bone. Pathology 14:439–442; 1982.
45. Zioupos, P., Wang, X. T., and Currey, J. D. Experimental and theoretical quantification of the development of damage in fatigue tests of bone and antler. J Biomech 29:989–1002; 1996.

Date Received: February 11, 1998
Date Revised: May 27, 1998
Date Accepted: May 28, 1998